CHEMISTRY OF MATERIALS
Communication

Chem. Mater. **2009,** *21,* 4353–4355 4353
DOI:10.1021/cm901127r

Surface Structure and Electronic Properties of In_2O_3(111) Single-Crystal Thin Films Grown on Y-Stabilized ZrO_2(111)

K. H. L. Zhang,*,† D.J. Payne,† R. G. Palgrave,† V. K. Lazarov,‡ W. Chen,§ A. T. S. Wee,§ C. F. McConville,# P. D. C. King,# T. D. Veal,# G. Panaccione,⊥ P. Lacovig,|| and R. G. Egdell†

†*Department of Chemistry, Chemistry Research Laboratory, University of Oxford, Mansfield Road, Oxford OX1 3TA, United Kingdom,* ‡*Department of Materials, University of Oxford, Parks Road, Oxford OX1 3PH, United Kingdom,* §*Department of Physics, National University of Singapore, Singapore 117542,* #*Department of Physics, University of Warwick, Coventry CV4 7AL, United Kingdom,* ⊥*Laboratorio TASC, INFM−CNR, Area Science Park, S.S. 14, Km 163.5, 34012 Trieste, Italy, and* ||*Sincrotrone Trieste, S.C.p.A., S.S. 14, Km 163, Area Science Park, I-34012 Trieste, Italy*

Received April 23, 2009
Revised Manuscript Received June 22, 2009

Transparent conducting oxides (TCOs) combine the properties of optical transparency in the visible region with a high electrical conductivity and are an essential component in liquid crystal displays and solar cells:[1,2] there is also a growing interest in "transparent electronics".[3−5] As one of the prototype TCOs, indium oxide (In_2O_3) is amenable to degenerate n-type doping with Sn cations to give so-called indium tin oxide (ITO). In spite of the growing technological importance of these materials, relatively little effort has been directed toward growth of single-crystal thin films of In_2O_3 or ITO.[6−11] Moreover, a fundamental understanding of bulk electronic structure is still in its infancy. For example, the bandgap of In_2O_3 has been widely quoted to be 3.75 eV, which marks the onset of strong optical absorption. A weaker absorption onset at 2.62 eV[12] has either been ignored[13] or attributed to indirect optical transitions.[12] However, ab initio band structure calculations on In_2O_3 found no evidence of the upward dispersion of the valence bands as required by this hypothesis.[14] Moreover, the fact that the valence band onset in photoemisssion is situated less than 3 eV below the Fermi energy is inconsistent with a bandgap of 3.75 eV, unless there is pronounced upward band bending at the surface.[15,16] Recently, it has been shown that the bandgap is in fact direct and the weak onset is due to dipole forbidden transitions.[17,18] Despite this advance of understanding, little is known about the surface atomic structure of In_2O_3. The surface structure, however, provides in turn the essential basis for understanding the surface electronic properties such as the band offset, which plays an important role in determining the potential performance and stability of devices.[19,20]

In_2O_3 adopts the body-centered cubic bixbyite structure, with space group *Ia*3 and lattice parameter a = 1.01170 nm.[21] The face-centered cubic fluorite structure of Y-stabilized ZrO_2 belongs to the space group *Fm*3*m* with lattice parameter a = 0.51423 nm at the 17% Y doping level of the substrates used in the current work.[22] Thus, there is a mismatch on the order of only 1.6% between 2a for Y-doped ZrO_2 (1.02846 nm) and a for In_2O_3. Moreover, the two structures involve similar cation arrays but with 1/4 of the anion sites of the fluorite structure vacant in In_2O_3. Thus, Y-doped ZrO_2 appears to be an ideal substrate for growth of well-ordered thin films of In_2O_3. However, in previous work on growth of In_2O_3 on (100) oriented Y-ZrO_2 by O-plasma-assisted molecular beam epitaxy (PAMBE), it has been found that there is a pronounced tendency for In_2O_3 films to break up into an array of square islands with sloping (111) side facets.[11] This is apparently driven by the lower energy of the (111) surface as compared with other low index surfaces and suggests that better quality growth may be achieved on (111) oriented substrates. Here we report the growth of In_2O_3(111) thin films on Y-doped ZrO_2(111) substrates by PAMBE. Ordered epitaxal growth was confirmed by high -resolution transmission electron microscopy (HRTEM). The surface geometrical structure was examined by atomic force microscopy (AFM), scanning tunnelling microscope (STM) and low electron energy diffraction (LEED), indicating an unreconstructed

*Corresponding author.

(1) Granqvist, C. G.; Hultåker, A. *Thin Solid Films* **2002**, *411*, 1.
(2) Granqvist, C. G. *Sol. Energy Mater. Sol. Cells* **2007**, *91*, 1529.
(3) Thomas, G. *Nature* **1997**, *389*, 907.
(4) Nomura, K.; et al. *Science* **2003**, *300*, 1269.
(5) Tsukazaki, A.; Ohtomo, A.; Kita, T.; Ohno, Y.; Ohno, H.; Kawasaki, M. *Science* **2007**, *315*, 1388.
(6) Chern, M. Y.; Hunag, Y. C.; Lu, X. L. *Thin Solid Films* **2007**, *515*, 7866.
(7) Wang, Ch. Y.; Dai, Y.; Pezoldt, J.; Lu, B.; Kups, Th.; Cimalla, V.; Ambacher, O. *Cryst. Growth Des.* **2008**, *8*, 1257.
(8) Ohta, H.; Orita, M.; Hirano, M.; Tanji, H.; Kawazoe, H.; Hosono, H. *Appl. Phys. Lett.* **2000**, *76*, 2740.
(9) Bourlange, A.; et al. *Appl. Phys. Lett.* **2008**, *92*, 092117.
(10) Morales, E. H.; He, Y.; Vinnichenko, M.; Delley, B.; Diebold, U. *New J. Phys.* **2008**, *10*, 125030.
(11) Bourlange, A.; Payne, D. J.; Egdell, R. G.; Foord, J. S.; Jacobs, R. M. J.; Schertel, A.; Dobson, P. J.; Hutchison, J. L. *Chem. Mater.* **2008**, *20*, 4551.
(12) Weiher, R. L.; Ley, R. P. *J. Appl. Phys.* **1966**, *37*, 299.
(13) Hamberg, I.; Granqvist, C. G.; Berggren, K. F.; Sernelius, B. E.; Egström, L. *Phys. Rev. B* **1984**, *30*, 3240.
(14) Erhart, P.; Klein, A.; Egdell, R. G.; Albe, K. *Phys. Rev. B* **2007**, *75*, 153205.
(15) Christou, V.; Etchells, M.; Renault, O.; Dobson, P. J.; Salata, O. V.; Beamson, G.; Egdell, R. G. *J. Appl. Phys.* **2000**, *88*, 5180.
(16) Gassenbauer, Y.; et al. *Phys. Rev. B* **2006**, *73*, 245312.
(17) Walsh, A.; et al. *Phys. Rev. Lett.* **2008**, *100*, 167402.
(18) Fuchs, F.; Bechstedt, F. *Phys. Rev. B* **2008**, *77*, 155107.
(19) Ishii, H.; Sugiyama, K.; Ito, E.; Seki, K. *Adv. Mater.* **1999**, *11*, 605.
(20) Khodabakhsh, S.; Sanderson, B. M.; Nelson, J.; Jones, T. S. *Adv. Funct. Mat.* **2006**, *16*, 95.
(21) Marezio, M. *Acta Crystallogr.* **1966**, *20*, 723.
(22) Moringa, M.; Cohen, J. B. *Acta Crystallogr., Sect. A* **1979**, *35*, 789.

Published on Web 09/01/2009

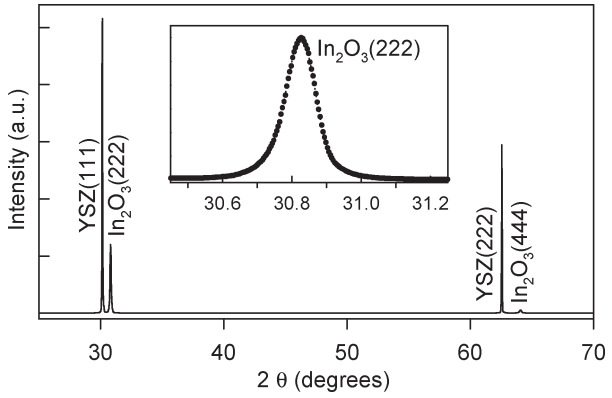

Figure 1. $\theta-2\theta$ X-ray diffraction profile of an In_2O_3 thin film grown on Y-ZrO_2(111).

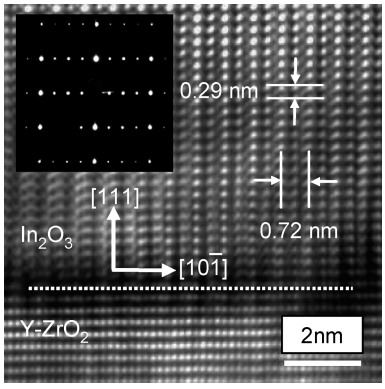

Figure 2. HRTEM image of the In_2O_3/Y-ZrO_2(111) interface viewed down the [$1\bar{2}1$] direction. The inset shows the corresponding diffraction pattern.

(1×1) surface termination. The comparison between the valence band edge spectra in photoemission excited at $h\nu = 1486.6$ eV and $h\nu = 6000.0$ eV reveals a pronounced accumulation of electrons close to the surface.

The In_2O_3 thin films were grown on 1 cm $\times$ 1 cm Y-stabilized ZrO_2(111) substrates in an ultrahigh vacuum oxide MBE system (SVT, USA) with a base pressure of 5×10^{-10} mbar. This incorporated a hot lip indium Knudsen cell and a radio frequency (RF) plasma oxygen atom source operated at 200 mW RF power with an oxygen background pressure of 3×10^{-5} mbar. Substrates were heated radiatively using a graphite filament. The nominal growth rate was 0.35 nm s^{-1} calibrated from the thickness from HRTEM measurements. The Y-ZrO_2 substrates were cleaned by exposure to the oxygen atom beam at a nominal substrate temperature of 900 °C. Films were then grown to a thickness of 210 nm at a substrate temperature of 700 °C. In situ LEED was carried out in an analysis chamber connected to the growth chamber. Cross-sectional HRTEM observations were carried out using a JEOL3000F microscope. AFM images were recorded with a tapping mode in a Digital Instruments Multimode SPM instrument. STM imaging was performed with a chemically etched W tip at 77 K in an Omicrometer LT-STM system interfaced with a Nanonis controller (Nanonis, Switzland). X-ray ($h\nu = 1486.6$ eV) photoemission spectra were recorded in a Scienta ESCA300 spectrometer with an effective instrument resolution of 0.40 eV. Hard X-ray photoemission spectra (HXPS) at $h\nu = 6000.0$ eV were measured on Beamline ID16 on the ESRF (Grenoble, France) with an overall energy resolution of 0.35 eV.

Figure 1 shows a representative $\theta-2\theta$ X-ray diffraction scan of a typical In_2O_3(111)/Y-ZrO_2(111) sample. Four peaks can be observed corresponding to the reflections of Y-ZrO_2(111), In_2O_3(222), Y-ZrO_2(222) and In_2O_3(444). This indicates a cubic In_2O_3 single-crystalline film with the [111] direction of the epilayer parallel to the [111] direction of Y-ZrO_2. The full width at half-maximum of the In_2O_3(222) peak (inset) is measured to be 0.115°, demonstrating the high crystal quality of the In_2O_3 epilayer. A cross sectional HRTEM image and the corresponding diffraction pattern taken from the substrate/epilayer interface are shown in Figure 2. The image shows an atomically abrupt interface with good registry between the epilayer and substrate. The epitaxial relationship is further confirmed by the coincidence between the substrate and epilayer spots in the selected area electron diffraction pattern taken across the interface. The atomic structure and interplanar separations marked on the images are consistent with the bixbyite structure of In_2O_3: the spacings of 0.72 and 0.29 nm are close to $a/\sqrt{2}$ and $a/2\sqrt{3}$, respectively.[21] The quality of the films is reflected in a very low carrier concentration (1.0×10^{18} cm^{-3}) and high mobility (56 cm^2 V^{-1} s^{-1}) as determined from single-field Hall effect measurements. Stoichiometric In_2O_3 should be a transparent insulator, but films prepared by sputtering or reactive electron beam evaporation[13,23] are almost invariably degenerate *n*-type semiconductors because of a high density of donor-type defects. Assuming a value of 8.9 for the static dielectric constant $\varepsilon(0)$ and an electron effective mass $m^* = 0.35m_0$ (where m_0 is the electron rest mass), the effective Bohr radius r_0^* for donor states is In_2O_3 is estimated to be 1.346 nm. The critical carrier concentration n_c for the onset of metallic conductivity as defined by the Mott criterion $(n_c)^{1/3}r_0^* > 0.26$ is calculated to be 7.21×10^{18} cm^{-3}. Our samples have carrier densities well below this limit.

Turning now to surface structure, Figure 3a shows a large area AFM topographic image. The surface is built up from atomically flat terraces but triangle shape islands are observed, reflecting the symmetry of a cubic (111) surface. The terraces are separated by atomic scale steps with a height of 0.3 ± 0.03 nm. This again corresponds to $a/2\sqrt{3}$, the same interplanar spacing as seen in HRTEM.

A typical in situ LEED pattern obtained from the In_2O_3(111) surface immediately after growth is presented as an inset to Figure 3a. It shows a sharp array of spots with 3-fold symmetry. The lattice constant is estimated to be 14.0 ± 0.5 Å, which is associated with the unreconstructed (1×1) surface structure of In_2O_3(111) where the cell side is equal to $\sqrt{2}a$, corresponding to the face diagonal of the bulk cell. Figure 3b shows a unit-cell-resolved

(23) Jeong, J. I.; Moon, J. H.; Hong, J. H.; Kang, J. S.; Y. Fukuda, Y.; Lee, Y. P. *J. Vac. Sci. Technol. A* **1996**, *14*, 293.

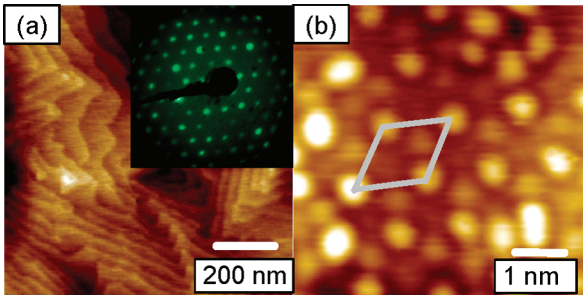

Figure 3. (a) Large area 1000 nm × 1000 nm AFM topographic image of the In_2O_3(111) thin film, showing staircases of atomic scale steps. The inset shows a corresponding LEED pattern obtained with 55.6 eV beam energy. (b) An atomically resolved empty state STM image (6 nm × 6 nm). The hexagonal surface (1 × 1) unit cell is indicated. $V_{tip} = -1.8$ V, I_t = 300 pA.

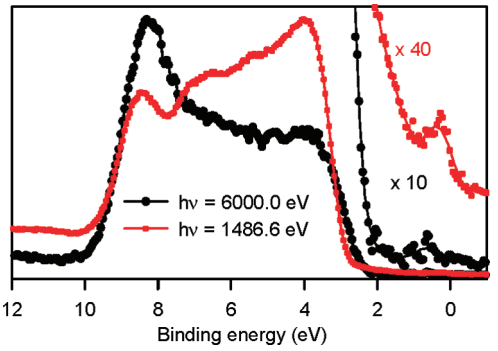

Figure 4. Valence band photoemission spectra of the epitaxial In_2O_3-(111) film. Al Kα $h\nu$ = 1486.6 eV (red) measured at 45° off-take angle and hard X-ray $h\nu$ = 6000 eV (black) measured at 90° off-take angle. The conduction band emission near the Fermi energy is magnified.

STM image, which was obtained after a few cycles of 500 eV Ar+ sputtering and 600 °C annealing in UHV. In contrast to previous work on Sn-doped In_2O_3 films, where the unit cell was defined by greyscale minima,[11] in our work the hexagonal surface cell is defined by topographic maxima. Subsidiary structure within the cell is also apparent. The side of the unit cell is again $\sqrt{2}a$, as expected.

Valence band photoemission spectra excited at $h\nu$ = 1486.6 eV (red) and $h\nu$ = 6000 eV (black) are shown in Figure 4. In the spectrum excited at 1486.6 eV (red), a well-defined peak is observed at the Fermi energy. However, this peak is much weaker in spectra excited at 6000 eV. In a previous study of In_2O_3(100) this feature was assigned to adventitious donor defects.[10] However the peak was later attributed to instrinic electron accumulation arising from pinning of the Fermi level at the surface about 0.4 eV above the conduction band mimimum: the pinning energy is assumed to lie close to the charge neutrality level.[24] The very low bulk carrier concentration in the present samples allows us to explore this idea further. Space charge calculations suggest that if the Fermi level is indeed pinned 0.4 eV above the conduction band minimum carrier accumulation takes place over a length range of about 5 nm. Assuming a "universal curve" mean free path (λ) of about 2 nm for photoelectrons with a kinetic energy close to 1.5 keV it can be shown that 97% of the photoelectron signal derives from the space charge region as defined above at 45° offtake angle. Thus Al Kα photoemission is dominated by the space charge region. By contrast in hard X-ray photoemission using 6 keV photons λ has been estimated to be about 6 nm.[25] Now the space charge region contributes significantly less (57%) to the total photoelectron signal at normal emission, with significant signal coming from the low carrier density "bulk" of the sample. Note that in comparing the conduction band intensities in Figure 4, we have applied an expansion to the Al Kα data that is a factor of 4 higher than to the HXPS data. This is to make allowance for the fact that the cross-section for ionization of In 5s states, which provide the major contribution to the conduction band, increases dramatically relative to the cross section for O 2p states at the higher photon energy.[26] We have shown[17] that for highly doped samples, where there is near flat band behavior, conduction band structure is indeed around a factor of 4 stronger relative to the maximum intensity in the O 2p valence band in HXPS at $h\nu$ = 6000 eV than in Al Kα XPS.

In summary, we have grown high-quality In_2O_3(111) thin films on Y-ZrO_2(111) by O plasma assisted molecular beam epitaxy. The films have unreconstructed In_2O_3-(111) (1 × 1) surfaces as determined by LEED and STM. The examination of valence band and conduction band spectra by HXPS adds further weight to the conclusion that the electron accumulation at the surface is an intrinsic property of In_2O_3.

Acknowledgment. K.H.L. Zhang is supported by the Oxford Clarendon Fund. We thank D.S.L. Law, G. Beamson, and L. Simonelli for technical assistance in XPS measurements. This work was supported by the EPSRC (UK) under Grants EP/E031595/1 (Warwick), GR/S94148 (Oxford), and EP/E025722/1 (XPS facility). This work has been supported in part by CNR-INFM.

Supporting Information Available: X-ray photoemission spectra of highly degenerate ITO thin films and Poisson-MTFA calculation diagrams of surface electron accumation layer (PDF). This material is available free of charge via the Internet at http://pubs.acs.org/.

(24) King, P. D. C.; Veal, T. D.; Payne, D. J.; Bourlange, A.; Egdell, R. G.; McConville, C. F. *Phys. Rev. Lett.* **2008**, *101*, 116808.
(25) Sachhi, M.; et al. *Phys. Rev. B* **2005**, *71*, 155117.
(26) Scofield, J. H. *Theoretical Photoionization Cross Sections from 1 to 1500 keV*; Lawrence Livermore National Laboratory Report UCRL-51326; Lawrence Livermore National Laboratory: Lawrence, CA, 1973.